OUKA
The University of Osaka
Institutional Knowledge Archive

| | |
|---|---|
| Title | TDM Intercell Connection Fiber-Optic Bus Link for Personal Radio Communication Systems |
| Author(s) | Harada, Hiroshi; Kajiya, Satoshi; Tsukamoto, Katsutoshi et al. |
| Citation | IEICE Transactions on Communications. 1995, E78-B(9), p. 1287-1294 |
| Version Type | VoR |
| URL | https://hdl.handle.net/11094/3444 |
| rights | copyright©2008 IEICE |
| Note | |

*The University of Osaka Institutional Knowledge Archive : OUKA*

https://ir.library.osaka-u.ac.jp/

The University of Osaka

PAPER

# TDM Intercell Connection Fiber-Optic Bus Link for Personal Radio Communication Systems

**Hiroshi HARADA†, Satoshi KAJIYA†, *Student Members*, Katsutoshi TSUKAMOTO†, Shozo KOMAKI†, *and* Norihiko MORINAGA†, *Members***

**SUMMARY** To connect among many radio base stations by using optical fiber bus link in microcellular system, subcarrier multiplexing (SCM) is excellent in simplicity and flexibility. But performance degradation due to optical beat noises is severe problem. To solve this problems, this paper proposes a new type of intercell connection bus fiber-optic link (ICBL) using time division multiplexing, called TDM-ICBL. This paper also analyzes transmission performance of TDM-ICBL theoretically and compares with SCM-ICBL. The analysis clarifies that while the number of RBSs connected to SCM-ICBL is severely restricted by beat noises, TDM-ICBL is more useful than SCM-ICBL when there are many number of connected RBSs.

***key words:*** *TDM, fiber-optic, bus link, bandpass sampling, optical beat interference*

## 1. Introduction

Future telecommunication trends are found both in personal communications and in global communications. Especially in mobile communication system, microcellular system, whose cell size is reduced to several 100 meters, has been proposed in order to cope with a rapid increase in the number of subscribers. The reduction in cell size improves the frequency utilization efficiency, reduces the power consumption of radio equipments and makes portable sets smaller. But this implementation needs the placement of many radio base stations (RBS) collecting and delivering RF signals and the effective connection among so many RBSs.

To solve these technical problems, it is proposed that microcells in wide area are connected by optical fibers and radio signals are transmitted over fiber-optic link among RBSs and a control station (CS). We can regard such a fiber-optic intercell connection link (ICCL) as a virtual free space for radio signals, and we call this system fiber and radio extension system (FREx Link) [1]-[7]. By employing FREx system, RBS is equipped only with an electric-to-optic converter (E/O) and an optic-to-electric converter (O/E), and all of the complicated functions such as RF modulation and demodulation, frequency assignment, spectrum delivery switching and so on, are performed at the CS. This system has the following features: flexible use of RBS's equipments for various types of service; high adsorbability for traffic fluctuation due to spectrum delivery switches centralized in the CS; low equipment cost for RBSs; and easy execution of handover among microcells. So, various researches on such optic-radio systems as FREx system are extensively performed in many countries [1]-[7].

Serious one of the problems in the implementation of FREx system is the configuration of fiber-optic links for ICCL. Conventionally, a single star configuration has been mainly investigated because of its high reliability and easy maintenance. However, a problem in this approach is the enormous investment for the construction of many fiber-optic links and also, the cost of optical transmitters and receivers equipped in the CS becomes burden. As an alternative configuration of ICCL, we have proposed the choice of the fiber-optic link with bus topology, named Intercell Connection fiber-optic Bus Link (ICBL) [6], [7]. In the ICBL system, since all RBSs of microcells share a fiber, the fiber count and the number of transmitter and receiver in the CS can be reduced, that is, the ICBL provides a cost effective approach for the implementation of FREx system.

FREx systems using subcarrier multiplexing (SCM) have been demonstrated [1]-[3]. Although SCM is excellent in simplicity and flexibility, if we choose SCM as a multiplexing scheme in the ICBL, the performance degradation due to optical beat noises is a severe problem at the CS's receiver [4]-[7]. These beat noises deteriorate the received carrier-to-noise ratio (CNR) performance drastically. Furthermore, in SCM-ICBL, a radio frequency used in one cell can't be reused in other cells because the CS can't distinguish between the optical signal from a specified RBS and those with the same frequency subcarrier from other RBSs. Therefore it is necessary to consider new multiplexing schemes suitable for ICBL.

In this paper, we propose newly ICBL using time division multiplexing called TDM-ICBL [7], where timewise sampled radio signals are transmitted and multiplexed over fiber-optic link. In TDM-ICBL, no beat noise arises and a radio frequency used in one cell can be reused in the other cell. In Sect. 2, the concept and configurations of ICBL are described. In Sect. 3,

Manuscript received October 31, 1994.
Manuscript revised March 13, 1995.

† The authors are with the Faculty of Engineering, Osaka University, Suita-shi, 565 Japan.

we analyze transmission performance of TDM-ICBL theoretically and in Sect. 4, we compare to SCM-ICBL and investigate the transmitter laser power reduction by the use of optical switches, theoretically.

## 2. Concept of Intercell Connection Fiber-Optic Bus Link (ICBL)

We propose ICBL (Intercell Connection fiber-optic Bus Link) with the configuration illustrated in Fig. 1. ICBL system connects among microcells with a fiber-optic bus link. At each radio base station (RBS) composed only of a LD and a few equipment, radio signals from subscribers are received, encapsulated into the envelope of optical signal by intensity modulation and transmitted to control station (CS) through a fiber-optic bus link.

To compensate the losses of couplers and fibers, optical amplifiers are equipped on ICBL at regular interval called sub-bus link, into which $M$ RBSs launch signal lights through optical couplers.

Figure 2 shows the configuration of a sub-bus link. A number of optical signals enter from the left

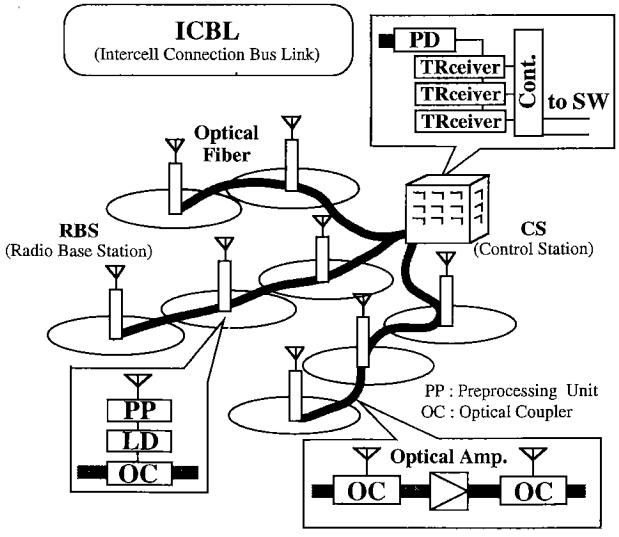


**Fig. 1** Concept of ICBL.

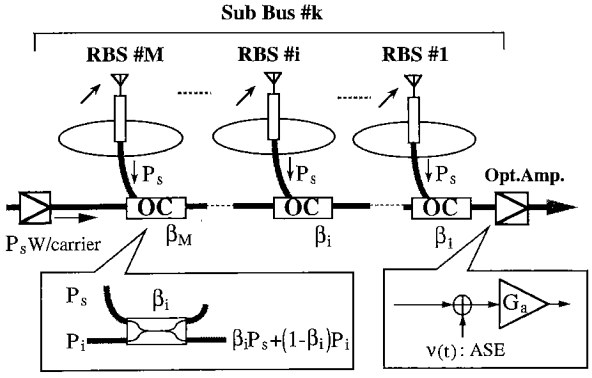


**Fig. 2** Configuration of sub-bus link.

end of a sub-bus link. Each signal is launched from different RBS included in the previous sub-bus links. We assumed that all these optical signals have the same power of $P_s$. Furthermore, assuming that the optical signal power launched by each of $M$ RBSs in this sub-bus link is $P_s$, we calculate the coupling coefficients of optical couplers to equalize all optical signal powers transmitted from RBSs included in all sub-bus links at this sub-bus output. When the coupling coefficient of $k$-th optical coupler is $\beta_k$ and the total loss of optical coupler and fiber is $\alpha_L$ [dB], the optical signal power transmitted from $i$-th RBS at the output of the sub-bus link, $P_{ri}$, is given by

$$P_{ri}=P_s 10^{-i\alpha_L/10}\prod_{k=1}^{i-1}(1-\beta_k)\,\beta_i \quad (i=1\cdots M), \tag{1}$$

and the optical signal transmitted from any RBS located in previous sub-bus links, which suffers the whole loss $\Lambda_s$ of a sub-bus link, has the output power $P_{through}$ given by

$$P_{through}=P_s\Lambda_s, \tag{2}$$

$$\Lambda_s=10^{-M\alpha_L/10}\prod_{k=1}^{M}(1-\beta_k). \tag{3}$$

Consequently, we can find the set of coupling coefficients to make all optical signal powers transmitted from RBSs equal at the output of this sub-bus link, i.e., $P_{r_1}=P_{r_2}=\cdots=P_{r_M}=P_{through}$, as the following equations:

$$\beta_M=\frac{10^{-\alpha_L/10}}{1+10^{-\alpha_L/10}}$$

$$\beta_i=\frac{\beta_{i+1}10^{-\alpha_L/10}}{1+\beta_{i+1}10^{-\alpha_L/10}} \quad (i=1\cdots M-1). \tag{4}$$

In this paper, it is also assumed that to overcome the whole loss of a sub-bus link, an optical amplifier is equipped at the output of the sub-bus link. Figure 2 also shows the model of an optical amplifier provided by a source of amplified spontaneous emission (ASE), $\nu(t)$, and an ideal noiseless amplifier with gain $G_a$ [8]. The power spectral density (PSD) of ASE, $N_{sp}$, is given by [8]

$$N_{sp}=\frac{\eta_{sp}}{\eta_a}\frac{G_a-1}{G_a}h\nu, \tag{5}$$

where $\eta_{sp}$ is the spontaneous emission factor, $\eta_a$ is the quantum efficiency of the amplifier and $h\nu$ is the photon energy. Then to compensate the whole loss of a sub-bus link, $\Lambda_s$, we set the gain of the optical amplifier, $G_a$, as

$$G_a=\frac{1}{\Lambda_s}. \tag{6}$$

For example when gain of optical amplifier is 20.5 dB and $\alpha=1$ [dB], a sub-bus link can connect 13 RBSs.

## 3. TDM Intercell Connection Bus Link

### 3.1 System Model

In ICBL, if we choose SCM as a multiplexing scheme, the RBS and the CS are constructed as illustrated in Fig. 3. In the SCM-ICBL, beat noises due to optical interaction arise in optical receiving process at the CS. Furthermore, a radio frequency used in one cell can't be reused in the other cells, because the CS can't receive simultaneously some optical signals modulated by the subcarrier with the same frequency at different RBSs.

In this paper we propose TDM intercell connection fiber-optic bus link (TDM-ICBL) with the configurations of RBS and CS illustrated in Fig. 4. For the uplink from RBS to CS, a radio signal received at RBS is timewise sampled and directly modulates the laser diode and in consequence, we obtain PAM/IM (Pulse Amplitude Modulation/optical Intensity Modulation) signal. Then the PAM/IM optical signal is fed into the optical bus link. In the optical bus link many PAM/IM signals launched by many RBSs are multiplexed by TDM and transmitted to the CS. At the CS all received optical PAM/IM signals are detected by a photodiode and then demultiplexed into one of each RBS by a distributor. Finally, by bandpass filtering the radio signal of each RBS is reconstructed from the demultiplexed PAM/IM signal. For the downlink from CS to RBS we operate the reverse.

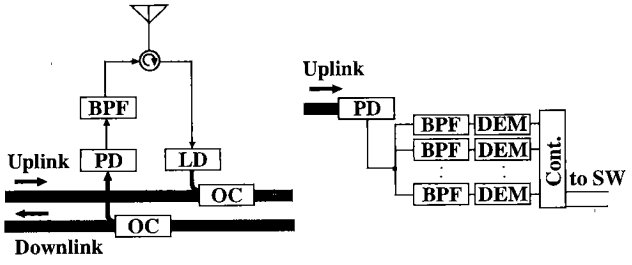


RBS (Radio Base Station) CS (Control Station)

**Fig. 3** Configurations of RBS and CS in SCM-ICBL.

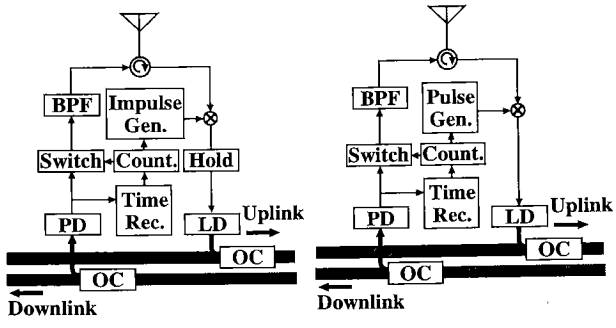


(a) Sampling-and-hold type (b) Window type

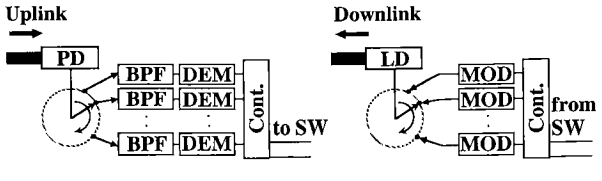


(c) CS (Control Station)

**Fig. 4** Configurations of RBS and CS in TDM-ICBL.

At the CS of TDM-ICBL, in contrast to SCM-ICBL, no optical beat noise arise and a radio frequency used in one cell can be reused in the other cell because optical signals from different RBSs are never received simultaneously.

In TDM-ICBL, a radio signal received at the RBS in each cell is timewise sampled to yield PAM signal. Then the PAM signals from each cell are time division multiplexed on the time slot assigned to each cell. Thus in this paper we assume that synchronous procedures of sampling and TDM are perfectly performed.

### 3.2 Bandpass Sampling

Figure 4 illustrates two types of RBS in TDM-ICBL. These systems are different in sampling method.

Figure 4(a) illustrates *sample-and-hold type* RBS, where a radio signal received at RBS, $g_k(t)$, is bandpass-timewise sampled [10] with sampling rate $f_s$ determined from radio carrier frequency $f_c$ and signal bandwidth $B_w$. The sampled signal is held and converted into PAM signal. Radio signal $g_k(t)$ received at $k$-th RBS with spectrum $G_k(f)$ is assumed by

$$g_k(t)=\mathrm{Re}[a(t)\,e^{j2\pi f_c t}], \tag{7}$$

$$G_k(f)=\frac{1}{2}[A(f-f_c)+A^*(-f-f_c)], \tag{8}$$

where $a(t)$ is a complex baseband information signal with bandwidth $B_w$ and $A(f)$ is the spectrum of $a(t)$.

The PAM signal $v_k(t)$ and its spectrum $V_k(f)$ are given by

$$v_k(t)=\sum_{n=-\infty}^{+\infty} g_k(nT_s)\,p(t-nT_s), \tag{9}$$

$$V_k(f)=\frac{T}{T_s}\mathrm{Sinc}(\pi Tf)\sum_{k=-\infty}^{+\infty} G_k(f-kf_s) \tag{10}$$

where sampling interval $T_s=1/f_s$ and $p(t)$ is a rectangular pulse with unit amplitude and pulse width of $T$. Figure 5(a) illustrates $V_k(f)$ given by Eq.(10). By bandpass sampling, $V_k(f)$ generates a series of $f_s$ shifted pattern of $G_k(f)$ to the left and to the right. And the energy of $A(f)$ is concentrated around $f=0$. Therefore, at CS of uplink, by filtering $v_k(t)$ around intermediate frequency $f_{IF}$ which sets $\mathrm{Sinc}(\pi f_{IF}T)$ to almost 1, we construct the radio signal with frequency $f_{IF}$ without down-convert.


(a) Sampling and hold type TDM-ICBL

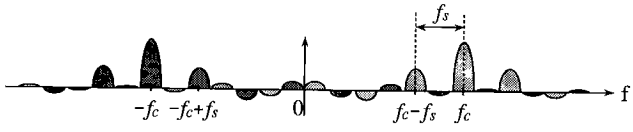


(b) Window type TDM-ICBL

**Fig. 5** Signal spectrum characteristics of TDM-ICBL.

In the above sampling process, we must avoid overlapping among the reproductions of $A(f)$ by using appropriate sampling rate $f_s$. The minimum sampling rate of bandpass-timewise sampling is given by [10]

$$f_{smin}=\frac{2}{M+1}(W_o+B_w), \tag{11}$$

where $W_o=f_c-B_w/2$ and $M$ is non negative maximum integer satisfying $M \leqq W_o/B_w$.

Figure 4(b), on the other hand, illustrates *window type* RBS, where a radio signal received at RBS, $g_k(t)$, is bandpass-timewise sampled by the multiplication with periodic pulse train, $s_p(t)$, given by

$$s_p(t)=\sum_{n=-\infty}^{+\infty} p(t-nT_s). \tag{12}$$

The PAM signal $v_k(t)$ and its spectrum, $V_k(f)$ are given by

$$v_k(t)=g_k(t)\times s_p(t) \tag{13}$$

$$V_k(f)=\frac{T}{T_s}\sum_{k=-\infty}^{+\infty}\mathrm{Sinc}(k\pi Tf_s)\,G_k(f-kf_s) \tag{14}$$

Figure 5(b) illustrates $V_k(f)$ given by Eq.(14). In this case, $V_k(f)$ is the arrangement of the reproductions of $A(f)$ as same as *sample-and-hold type*. However, the energy of $A(f)$ is concentrated around $|f|=f_c$. Therefore, if we apply this system to downlink, we can easily construct the radio signal with frequency $f_c$ without upconversion in contrast to the *sample-and-hole type*.

### 3.3 Theoretical Analysis of Received CNR

Assuming that one radio carrier is used in each microcell and multiplexes all users in each cell, we theoretically analyze the received CNR of the radio signal reproduced at the CS of uplink.

The PAM signal produced from $g_k(t)$ at the $k$th RBS, $v_k(t)$, directly intensity-modulates the LD and the obtained PAM/IM signal is time-division-multiplexed with other RBS's signals. TDM optical PAM/IM signal received at the CS is written by

$$I_r(t)=P_r(1+v_{IM}(t)), \tag{15}$$

$$v_{IM}(t)=\sum_{k=0}^{N_c}\sum_{n=-\infty}^{+\infty} g_k(nT_s)\,p(t-nT_s-kT), \tag{16}$$

where $P_r$ is the average received optical power, and $N_c$ is the total number of RBS included in the whole system, and we assume $|v_{IM}(t)|\leqq 1$, e.g., $|a(t)|\leqq 1$. $R_r$ is given by

$$P_r=\frac{P_s}{F_{loss}}, \tag{17}$$

where $P_s$ is the transmitted power of each RBS's LD and $F_{loss}$ is the fiber loss between the CS and the most adjacent optical coupler to CS. The output current of PD in CS is given by

$$i_{out}(t)=\alpha P_r(1+v_{IM}(t))+n(t), \tag{18}$$

where $\alpha$ is the responsibity of PD and $n(t)$ is given as

$$n(t)=i_{RIN}(t)+i_{shot}(t)+i_{th}(t)+i_{s-sp}(t)+i_{sp-sp}(t), \tag{19}$$

where $i_{RIN}(t)$, $i_{shot}(t)$, $i_{th}(t)$, $i_{s-sp}(t)$ and $i_{sp-sp}(t)$ are the relative intensity noise current, shot noise current, receiver thermal noise current, beat noise current among ASEs and optical signal and beat noise current among ASEs, respectively. The noise current $n(t)$ is modeled as white gaussian noise process with one-sided PSD $n_o$ given by

$$n_o=n_{RIN}+n_{shot}+n_{th}+n_{s-sp}+n_{sp-sp}, \tag{20}$$

where

$$n_{RIN}=(\alpha P_r)^2 RIN, \tag{21}$$

$$n_{shot}=2e\alpha(P_r+mN_{sp}B_o), \tag{22}$$

$$n_{th}=\frac{4k\theta}{R}, \tag{23}$$

$$n_{s-sp}=4\alpha^2 mP_rN_{sp}, \tag{24}$$

$$n_{sp-sp}=2\alpha^2(mN_{sp})^2(B_o-f_c), \tag{25}$$

where $RIN$, $m$, $B_o$, $e$, $k$, $R$ and $\theta$ are the PSD of relative intensity noise, the number of optical amplifier, the bandwidth of optical filter at the CS, electron charge, Boltzman constant, load resistance and noise temperature, respectively. In Eq.(20), $n_{th}$ and $n_{sp-sp}$ are signal-independent noises and the others are signal-dependent noises. Generally, as $P_r$ increases, signal-dependent noises become dominant. Next, the distributor separates PAM signals from the output current, $i_{out}(t)$, and distributes them to a bank of BPFs and demodulators illustrated in Fig. 4(c). The $k$-th outputs of distributor is given by

$$i_k(t)=\sum_{l=-\infty}^{+\infty} i_{out}(t)\,p(t-lT_s-kT)$$

$$= v_{PAM}(t) + n_{PAM}(t), \quad (26)$$

where the first term $v_{PAM}(t)$ is the demultiplexed PAM signal of $k$-th RBS given by

$$v_{PAM}(t) = \sum_{l=-\infty}^{+\infty} \alpha P_r (1 + v_{IM}(t)) p(t - lT_s - kT), \quad (27)$$

and the second term $n_{PAM}(t)$ is given by

$$n_{PAM}(t) = n(t) \times s_p(t), \quad (28)$$

The autocorrelation function of $n_{PAM}(t)$ is given by

$$R_{PAM}(\tau) = R_p(\tau) \times R_n(\tau), \quad (29)$$

where the autocorrelation function of $s_p(t)$, $R_p(\tau)$, is given by

$$R_p(\tau) = \sum_{k=-\infty}^{+\infty} f(\tau - kT_s), \quad (30)$$

$$f(\tau) = \begin{cases} \dfrac{T - |\tau|}{T_s}; & |\tau| \leqq T \\ 0 \quad ; \text{ otherwise.} \end{cases} \quad (31)$$

and further, since $n(t)$ is white gaussian noise process, $R_n(\tau)$ is given by $(n_o/2)\,\delta(\tau)$, where $\delta(\tau)$ is a delta function. Therefore the autocorrelation function $R_{PAM}(\tau)$ and the PSD of $n_{PAM}(t)$, $S_{PAM}(f)$, are given as

$$R_{PAM}(\tau) = \frac{T - |\tau|}{T_s} \cdot \frac{n_o}{2} \delta(\tau), \quad (32)$$

$$S_{PAM}(f) = \frac{T}{T_s} \cdot \frac{n_o}{2}. \quad (33)$$

Finally, by only bandpass filtering, we reconstruct the radio signal of $k$-th RBS, $g_k(t)$ with frequency $f_{IF}$. Assuming ideal BPF with the transfer function $H_{IF}(f)$ given as

$$H_{IF}(f) = \begin{cases} 1; & |f - f_{IF}| \leqq \dfrac{B_w}{2} \\ 0; & \text{otherwise,} \end{cases} \quad (34)$$

the reconstructed $k$-th radio signal, $\hat{g}_k(t)$, is given by

$$\hat{g}_k(t) = \frac{T}{T_s} \alpha P_r \,\mathrm{Sinc}(\pi f_{IF} T)\,\mathrm{Re}[a(t)\, e^{j2\pi f_{IF} t}]. \quad (35)$$

If we choose the intermediate frequency $f_{IF}$ which sets $\mathrm{Sinc}(\pi f_{IF} T)$ to almost 1, the carrier power of $\hat{g}_k(t)$ is given by

$$\langle I_s^2 \rangle = \frac{1}{2} \left( \frac{T}{T_s} \right)^2 (\alpha P_r)^2. \quad (36)$$

From Eqs. (33) and (36), consequently, the received CNR of reconstructed ratio signal at the CS is derived as

$$\left( \frac{C}{N} \right)_{TDM} = \frac{\langle I_s^2 \rangle}{\frac{T}{T_s} \frac{n_o}{2} 2B_w} = \frac{1}{2} \frac{T}{T_s} \frac{(\alpha P_r)^2}{n_o B_w}. \quad (37)$$

## 4. The Performance of TDM-ICBL

### 4.1 Comparison with SCM-ICBL

In the following, the performances of the proposed TDM-ICBL are compared to conventional SCM-ICBL. Both the SCM- and the TDM-ICBL have the same fiber-link configuration shown in Fig. 1, which is composed of some sub-bus links shown in Fig. 2. The configurations of the RBS units connecting with the SCM-ICBL and the TDM-ICBL are shown in Fig. 3 and Fig. 4, respectively. And at the CS the received CNR of radio signal transmitted from each of RBSs is given as follows [6].

$$\left( \frac{C}{N} \right)_{SCM} = \frac{\frac{1}{2} m_{opt}^2 (\alpha P_r)^2}{n_o B_w + \overline{\langle I_{s-s}^2 \rangle}}, \quad (38)$$

where $n_o$ is given by Eq. (20). But in SCM-ICBL, radio signals transmitted from each of $N_c$ RBSs and ASE signals transmitted from each of $m$ optical amplifiers are received at the CS. Therefore $n_{RIN}$, $n_{shot}$, $n_{th}$, $n_{s-sp}$ and $n_{sp-sp}$ shown in Eq. (20) are given by

$$n_{RIN} = \sum_{k=1}^{N_c} RIN (\alpha P_{rk})^2, \quad (39)$$

$$n_{shot} = 2e\alpha \left\{ \sum_{k=1}^{N_c} P_{rk} + mN_{sp}W \right\}, \quad (40)$$

$$n_{th} = \frac{4k\theta}{R}, \quad (41)$$

$$n_{s-sp} = 4\alpha^2 \sum_{k=1}^{N_c} P_{rk} mN_{sp}, \quad (42)$$

$$n_{sp-sp} = 2\alpha^2 (mN_{sp})^2 (B_o - f_o), \quad (43)$$

where it is assumed that optical intensity modulation index $m_{opt}$ is set to be 1 and $P_{rk} = P_r$ $(k = 1, 2, \cdots, N_c)$. $\langle i_{s-s}^2 \rangle$ is the average power of optical signal-signal beat noise.

While non-modulated output light of LD has Lorentzian-shaped spectrum, the spectrum of the output light modulated by a radio frequency carrier has a periodical Lorentzian-shaped spectrum. Taking into account this spectrum spread, this paper assumes that the spectrum of the modulated LD output light at $i$-th RBS has the gaussian shaped spectrum with the spectral linewidth (full-width-half-maximum) of $\Delta\nu_i$ and the center frequency of $f_{oi}$. The power of optical signal-signal beat noise is given by [6]

$$\langle I_{s-s}^2 \rangle = \alpha^2 \sum_{i=1}^{N_c} \sum_{\substack{k=1 \\ i \neq k}}^{N_c} P_r^2 \left[ \mathrm{erfc} \left\{ \frac{-2(f_c + \delta f_{ik}) - B_w}{2\sqrt{2}\sigma_{ik}} \right\} \right.$$

$$-\mathrm{erfc}\left\{\frac{-2(f_c+\delta f_{ik})+B_w}{2\sqrt{2}\sigma_{ik}}\right\}$$
$$+\mathrm{erfc}\left\{\frac{-2(f_c-\delta f_{ik})-B_w}{2\sqrt{2}\sigma_{ik}}\right\}$$
$$-\mathrm{erfc}\left\{\frac{-2(f_c-\delta f_{ik})+B_w}{2\sqrt{2}\sigma_{ik}}\right\}\Bigg], \quad (44)$$

where

$$\delta f_{ik}=f_{oi}-f_{ok}, \quad \sigma_{ik}^2=\sigma_i^2+\sigma_k^2,$$
$$\sigma_i=\frac{\Delta\nu_i}{2\sqrt{2\log 2}} \quad (i, k=1, 2, \cdots, N_c),$$

and $\Delta\nu_i$ is the spectral linewidth of the optical carrier transmitted from $i$-th RBS. Equation (44) shows that $\langle i_{s-s}^2\rangle$ is dependent on $\delta f_{ik}$. Assuming that the optical carrier frequencies, $f_{oi}$ $(i=1, 2, \cdots, N_c)$, are mutually independent random variables with mean of $f_o$ and uniform probability density in the range $|f_{oi}-f_o|\leqq \Delta f/2$, the p.d.f of $\delta f_{ik}$ is given by

$$p(\delta f_{ik})=\begin{cases}\dfrac{1}{(\Delta f)^2}(\Delta f-|\delta f_{ik}|); & |\delta f_{ik}|\leqq\Delta f\\ 0 & ; |\delta f_{ik}|>\Delta f.\end{cases} \quad (45)$$

By using Eqs. (44) and (45), the ensemble average of optical signal-signal beat noise power, $\overline{\langle i_{s-s}^2\rangle}$, is given by

$$\overline{\langle i_{s-s}^2\rangle}=\int_{-\Delta f}^{\Delta f}\langle i_{s-s}^2\rangle p(\delta f_{ik})\, d\delta f_{ik}. \quad (46)$$

The CNR performances of SCM- and TDM-ICBL (Eqs. (37) and (38)) are discussed below with parameters indicated in Table 1. By $G_a=20.5$ dB, in this case, we mean that thirteen RBSs per one sub-bus link can be connected from Eqs. (3), (4) and (6) in Sect. 2.

Figure 6 show the relationship between the number of RBSs connected on ICBL and received optical signal power required to obtain the received CNR of 20 dB at CS. In the CNR of SCM-ICBL, the laser frequency variance $\Delta f$ and the laser linewidth $\Delta\nu$ are varied as parameter.

This figure shows that when the number of connected RBSs are small, SCM-ICBL requires smaller received power than TDM-ICBL. In SCM-ICBL, however, as RBS's number increases, required optical power of SCM-ICBL increases suddenly due to signal-signal beat noises, and as $\Delta f$ or $\Delta\nu$ decreases, the number of connected RBSs is more and more restricted, because the beat noise spectrum is concentrated on the radio frequency bandwidth when $\Delta f$ and $\Delta\nu$ decreases.

In TDM-ICBL, on the other hand, although optical signal power at the CS increases in proportion to the number of RBSs, the number of connected RBSs is never restricted. Therefore TDM-ICBL is useful when there are many RBSs or when lasers with small $\Delta f$ or narrow $\Delta\nu$ are used.

**Table 1** Parameters used in calculation.

| | | | | | |
|---|---|---|---|---|---|
| $RIN$ | -152dB/Hz | $\lambda$ | 1.53$\mu$m | $\eta_{sp}$ | 2.0 |
| $\eta_a$ | 0.5 | $G_a$ | 20.5dB | $\alpha$ | 0.8A/W |
| $B_w$ | 2MHz | $f_c$ | 1.5GHz | $B_o$ | 1THz |
| $R$ | 50$\Omega$ | $\theta$ | 300K | $\alpha_L$ | 1dB |

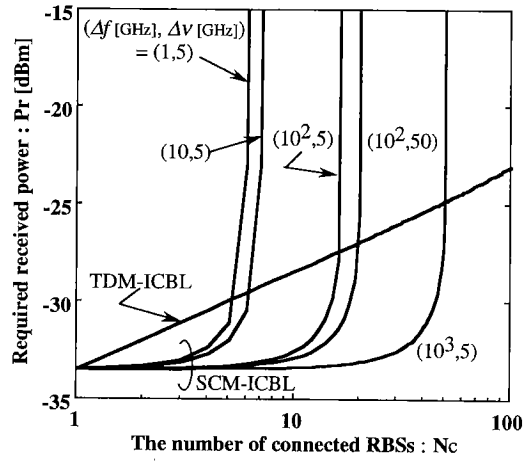


**Fig. 6** Relationship between the number of connected RBSs and $P_r$.

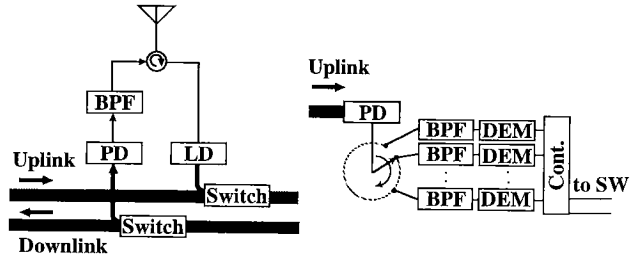


RBS (Radio Base Station) CS (Control Station)

**Fig. 7** Configurations of RBS and CS for switching type TDM-ICBL.

## 4.2 Use of Optical Switch to Reduce the Transmitted Laser Power

In the TDM-ICBL, an optical switch can simultaneously perform both the timewise sampling and the time-division-multiplexing in the bus-link as shown in Fig. 7. In this case, the received signal shape is the same as *window type* RBS. By using optical switches, it is expected that high sampling rate is available. Therefore we obtain high reliability of received signal. And the received CNR as a function of transmitting laser power at RBS, $P_s$, is calculated and the results are

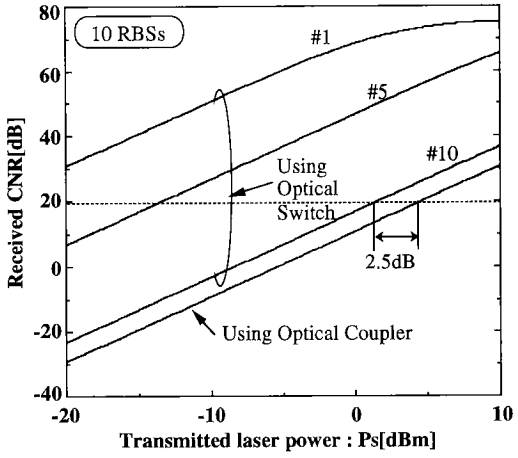


**Fig. 8** Received CNR as a function of transmitted laser power at RBS ($\alpha_L = \alpha_s = 3$ dB).

shown in Fig. 8. In the analysis, for the both cases of using couplers and using switches, it is assumed that 10 RBSs are connected to TDM-ICBL without optical amplifier and also assumed that the insertion loss of an optical switch, $\alpha_s$, is equal to one of optical coupler $\alpha_L$. This figure shows that by using optical switches, the transmitting laser power of the RBS of TDM-ICBL can be reduced in addition to previous features. For example, even for the farthest RBS (RBS # 10) from CS, transmitter laser power can be reduced by 2.5 dB than the case of using couplers to obtain received CNR of 20 dB at CS, because in the case of using couplers the received signal at CS suffers more coupling loss in the coupler than in the switch as shown in Eq.(1). Therefore by using optical switches, it is expected to obtain higher quality of received signal than the case of using couplers.

## 5. Conclusion

In this paper, we have newly proposed TDM intercell connection fiber-optic bus link for microcellular personal radio communication system. We analyzed CNR performances of TDM-ICBL and compared them with SCM-ICBL theoretically and further, considered the use of optical switches. As results, followings are obtained:

The number of RBSs connected on SCM-ICBL is severely restricted because of large optical signal-signal beat noises. On the other hand, in TDM-ICBL, though required optical signal power increases in proportion to the number of RBSs, the number of RBSs connected on TDM-ICBL is never restricted. And the use of optical switches for TDM-ICBL is effective for the laser power reduction in the RBSs.

## References

[1] S. Komaki, K. Tsukamoto, S. Hara, and N. Morinaga, "Proposal fiber and radio extension link for future personal communications," Microwave and Optical Technology Letters, vol. 6, no. 1, pp. 55-60, Jan. 1993.

[2] M. Shibutani, T. Kanai, K. Emura, and J. Namiki, "Feasibility studies on an optical fiber feeder system for microcellular mobile communication systems," Proc. ICC'91, pp. 1176-1181, June 1991.

[3] W. I. Way, "Subcarrier multiplexed lightwave system design considerations for subcarrier loop applications," IEEE J. Lightwave Tech., vol. 7, no. 11, pp. 1806-1818, Nov. 1989.

[4] N. K. Shankaranarayanan, S. D. Elby, and K. Y. Lau, "WDMA/subcarrier-FDMA ligitwave networks: Limitations due to optical beat interference," IEEE J. Lightwave Tech., vol. 9, no. 7, pp. 931-943, July 1991.

[5] Y. Tarusawa and T. Nojima, "C/N improved analog optic-fiber transmission by wavelength offset combining," Proc. IEICE Fall Conf. '93, B-336, Sep. 1993.

[6] T. Fujii, K. Tsukamoto, and N. Morinaga, "Transmission characteristics analysis of optical fiber bus link with optical amplifier for microcellular communication systems," IEICE Technical Report, RCS92-76, Oct. 1987.

[7] S. Kajiya, H. Harada, K. Tsukamoto, and S. Komaki, "TDM optical fiber bus link for microcellular radio communication system," Proc. IEICE Spring Conf. '94, B-325, Mar. 1994.

[8] S. S. Wagner, "Optical amplifier applications in fiber-optic local networks," IEEE Trans on Commun., vol. 35, no. 4, pp. 419-426, 1987.

[9] N. A. Olsson, "Lightwave systems with optical amplifiers," IEEE J. Lightwave Tech., vol. 7, no. 7, pp. 726-740, July 1989.

[10] A. Kohlenberg, "Exact interpolation of band-limited functions," J. Appl. Phys., vol. 24, no. 12, pp. 1432-1436, Dec. 1987.

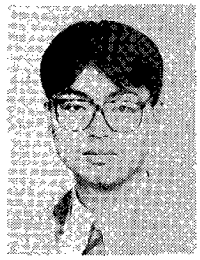

**Hiroshi Harada** was born in Kobe, Japan, on December 28, 1969. He received M.E. and Ph.D. degrees in Communication Engineering from Osaka University, Osaka, Japan, in 1994 and 1995 respectively. He joined Communications Research Laboratory, Ministry (CRL) of Posts and Telecommunications Japan, in 1995. He was engaged in the research on radio and optical communication systems in Osaka University. Dr. Harada is a member of IEEE.

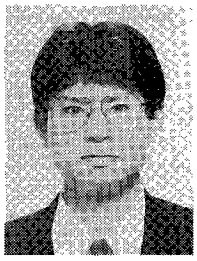

**Satoshi Kajiya** was born in Kagoshima, Japan, on March 23, 1971. He received the B.E. degree in Electrical Engineering from Osaka University, Osaka, Japan, in 1994. He is currently pursuing the M.E. degree at Osaka University. He is engaging in research on radio and optical communication systems.

**Katsutoshi Tsukamoto** was born in Shiga, Japan in October 7, 1959. He received the B.E. and M.E. degrees in Communication Engineering from Osaka University, in 1982 and 1984 respectively. He is currently a Research Assistant in the Department of Electrical Engineering at Osaka University, engaging in the research on radio and optical communication systems. He is a member of IEEE.

**Shozo Komaki** was born in Osaka, Japan, in 1947. He received B.E., M.E. and Ph.D. degrees in Electrical Communication Engineering from Osaka University, in 1970, 1972 and 1983 respectively. In 1972, he joined the NTT Radio Communication Labs., where he was engaged in repeater development for a 20-GHz digital radio system, 16-QAM and 256-QAM systems. From 1990, he moved to Osaka University, Faculty of Engineering, and engaging in the research on radio and optical communication systems. He is currently a Professor of Osaka University. Dr. Komaki is a senior member of IEEE, and a member of the Institute of Television Engineers of Japan (ITE). He was awarded the Paper Award and the Achievement Award of IECE, Japan in 1977 and 1994 respectively.

**Norihiko Morinaga** was born in Nishinomiya, Japan, on June 6, 1939. He received the B.E. degree in electrical engineering from Shizuoka University, Shizuoka, Japan, in 1963, and M.E. and Ph.D. degrees from Osaka University, Osaka, Japan, in 1965 and 1968 respectively. He is currently a Professor in the Department of Communication Engineering at Osaka University, working in the area of radio, mobile, satellite and optical communication systems, and EMC. Dr. Morinaga is a senior member of the IEEE and the Institute of Television Engineers of Japan.